

11-22-2020

Natural Convection Heat Transfer from Discrete Heat Sources Mounted in Rectangular Enclosure Surrounded by a Single-Phase Liquid Coolant.

S. El-agouz

Faculty of Engineering., Tanta University., Egypt.

M. Bekheit

Faculty of Engineering., El-Mansoura University., Egypt.

A. Kabeel

Faculty of Engineering., Tanta University., Egypt., kabeel6@yahoo.com

Follow this and additional works at: <https://mej.researchcommons.org/home>

Recommended Citation

El-agouz, S.; Bekheit, M.; and Kabeel, A. (2020) "Natural Convection Heat Transfer from Discrete Heat Sources Mounted in Rectangular Enclosure Surrounded by a Single-Phase Liquid Coolant.," *Mansoura Engineering Journal*: Vol. 35 : Iss. 1 , Article 27.

Available at: <https://doi.org/10.21608/bfemu.2020.124701>

This Original Study is brought to you for free and open access by Mansoura Engineering Journal. It has been accepted for inclusion in Mansoura Engineering Journal by an authorized editor of Mansoura Engineering Journal. For more information, please contact mej@mans.edu.eg.

Natural convection heat transfer from discrete heat sources mounted in rectangular enclosure surrounded by a single-phase liquid coolant

انتقال الحرارة بالحمل الطبيعي من مصادر حرارية مثبتة داخل مستطيل مغلق ومحاطه بسائل تبريد احادي الطور

S. A. El-agouz*, M.M. Bekheit**, A.E. Kabeel*

*Faculty of Engineering, Tanta University, Egypt.

**Faculty of Engineering, Mansoura University, Egypt.

الخلاصة:

يقدم هذا البحث دراسة معملية وعددية لانتقال الحرارة بالحمل الطبيعي من مصادر حرارية مثبتة داخل حيز لتمثيل تبريد الأجهزة الإلكترونية باستخدام السوائل. من أجل ذلك تم تصميم جهاز معمل يتكون من ثلاث مصادر حرارية داخل حيز وضع فيه سائل تبريد عبارة عن الماء أو زيت محول كهربائي. تم حساب توزيع درجات الحرارة عن طريق حل المعادلات الحاكمة مع استخدام نموذج $k-\epsilon$ ودالة الجدار عددياً. ركزت الدراسة على دراسة تأثير نوع سائل التبريد وكمية الفيض الحراري والزمن على درجات حرارة للمصادر الحرارية. اوضحت الدراسة فعالية تبريد المصادر الحرارية بالسائل كما اوضحت أن توزيع درجات الحرارة للماء تعطى نتائج افضل عنها عند استخدام الزيت (زيت محول كهربائي) في التبريد. وجد توافق بين النتائج المعملية والنظرية مرضية.

Abstract

In the present work, natural convection heat transfer from discrete heat sources mounted in rectangular enclosure using liquid coolant is investigated. Heat transfer from discrete heaters is non-uniform and should be accounted for by applying the averaging techniques. The averaged two-dimensional governing equations along with the standard $k-\epsilon$ model and wall function are solved using the SIMPLE algorithm. The effects of the cooling fluid type water and dielectrics oil, the different heat flux and time on heat transfer are investigated. The results are compared with experimental measurements. Results show that water gives a good cooling effect compared with dielectrics oil. Maximum heat transfer occurs at the heater leading and side edges. The heater surface temperature is highest at the top-row heaters. Results show also good agreement between the theoretical and experimental measurements.

Keywords: Discreate heat sources, Heat Transfer, Electronics cooling

Introduction

There is increasing demand for high performance and multiple functions in electronic systems. The cooling of electronic parts has become a major challenge in recent times due to the advancements in the design of faster and smaller components. Devices continue to present great challenges in their

thermal management. Conventional air cooling techniques are reaching their limits for applications in areas such as cost-performance and high performance electronics. Single-phase and two-phase liquid cooling techniques with heat sinks provide an approach for removing heat fluxes well beyond air cooling limits.

Natural convection heat transfer is an important phenomenon in engineering systems due to its wide application in electronics cooling, heat exchangers, and double pane windows. Enhancement of heat transfer in these systems is essential from the industrial and energy saving perspectives. The low thermal conductivity of conventional heat transfer fluids, such as water puts a primary limitation on the performance and the compactness of thermal systems. As a result, different cooling technologies have been developed to efficiently remove the heat from these components. The use of a liquid coolant has become attractive due to the higher heat transfer coefficient achieved as compared to air-cooling. Coolants are used in both single phase and two-phase applications. A single phase cooling loop consists of a pump, a heat exchanger (cold plate/mini- or micro-channels), and a heat sink (radiator with a fan or a liquid-to-liquid heat exchanger with chilled water cooling). The heat source in the electronics system is attached to the heat exchanger. Liquid coolants are also used in two-phase systems, such as heat pipes, thermo-siphons, sub-cooled boiling, spray cooling, and direct immersion systems for cooling of electronics [1]

The rapid development in the design of electronic packages for modern high-speed computers has led to the demand for new and reliable methods of chip cooling. As stated by Mahalingam and Berg [2], the averaged dissipating heat flux can be up to 25 W/cm^2 for high-speed electronic components. However, the conventional natural or forced convection cooling methods are only capable of removing small heat fluxes per unit temperature difference, about $0.001 \text{ W/cm}^2 \text{ C}$ by natural convection to air, $0.01 \text{ W/cm}^2 \text{ C}$ by forced convection to air, and $0.1 \text{ W/cm}^2 \text{ C}$ by forced convection to single-phase liquid [3]. In response to these demands, different highly effective cooling

techniques have been used to achieve heat transfer enhancement with a minimum of frictional losses, including a variety of passive and active cooling techniques.

Po-Chuan Huang and young [4] conducted a numerical investigation on the flow field and heat transfer characteristics of two successive porous-block mounted heat sources subjected to pulsating channel flow. Time-dependent flow and temperature fields were calculated and averaged over a pulsating cycle in a periodic steady-state. The basic interaction phenomena between the porous substrate and the fluid region, as well as the action of pulsation on the transport process were scrutinized within the study. Steady-state experiments were performed to study general convective heat transfer from an in-line four simulated electronic chips in a vertical rectangular channel using water as the working fluid [5]. Experiment has been performed to investigate the natural convection heat transfer coupled with the effect of thermal conduction from a steel plate with discrete heat sources. The behavior and heat transfer enhancement of a particular nanofluid, Al_2O_3 nanoparticle-water mixture, flowing inside a closed system that is destined for cooling of microprocessors or other electronic components was investigated by Cong Tam Nguyen et al [6]. The development of a novel cooling strategy of directly injected cooling for electronic packages was studied by Wits et al [7]. Two-dimensional forced convection heat transfer between two plates with flush-mounted discrete heat sources on one plate to simulate electronics cooling is studied numerically using a finite difference method in [8]. The effects of rotation on natural convection cooling from three rows of heat sources in a rectangular cavity were studied by Jin et al [9]. Conjugate convective-conductive heat transfer in a rectangular enclosure under the condition of mass transfer within cavity with local heat

and contaminant sources is numerically investigated by Kuznetsov and Sheremet [10]. Mathematical model, describing a two-dimensional and laminar natural convection in a cavity with heat-conducting walls, is formulated in terms of the dimensionless stream function, vorticity, temperature and solute concentration. The main attention is paid to the effects of Grashof number (Gr), Buoyancy ratio (Br) and transient factor on flow modes, heat and mass transfer.

Steady-state experiments are performed to study general convective heat transfer from an in-line four simulated electronic chips in a vertical rectangular channel using water as the working fluid [11]. Numerical simulation of conjugate, turbulent mixed convection heat transfer in a vertical channel with discrete heat sources was studied by Mathews and Balaji [12]. Investigation of mixed convection heat transfer in a horizontal channel with discrete heat sources at the top and at the bottom was studied by Dogan et al [13]. Laminar-mixed convection of a dielectric fluid contained in a two-dimensional enclosure is investigated [14]. Spray cooling is a very complex phenomena that is of increasing technological interest for electronic cooling and other high heat flux applications since much higher heat transfer rates compared to boiling can be achieved using relatively little fluid [15]. An experimental study of cooling an array of multiple heat sources simulating electronic equipment by a single row of slot air jets positioned above a critical row (row having maximum heat dissipation rate) of the array was conducted [16]. Kabeel et al [18] presented forced convection cooling of heat sources by use liquid (water and dielectrics oil). The study was carried out at different exit conditions, different flow rate, and different heat flux. Also, the study presented the effect of outlet ports positions for water and dielectrics oil to investigate the best position of exit flow. Although earlier works

have studied the use of liquid to enhance heat transfer from heat sources, they present few cases of this use.

In the present study, IC's components "chips" is idealized as smooth rectangular blocks with uniform thermal conductivity and constant heat flux. The aim of the present work is to use liquid (water and dielectrics oil) to cooling heat sources. Turbulent heat transfer with three heat sources for liquid coolant water and dielectrics oil is studied experimentally and numerically. The present results are compared with relevant experimental data. The effects of the type fluid cooling and the different heat flux on heat transfer are investigated.

Experimental test rig

The details of the experimental test rig are shown in Fig. 1. It consists of the cooling chamber (1), thermocouples (3), temperature indicator (5), Ammeter (6), Voltage transformer (Variac) (8) and power supply.

The test section consists of two parts that are the cooling chamber (1) and the chips (2) as shown in Fig. 2. The cooling chamber (1) is made of Acrylic with of 1 mm thickness, width of 102 mm, height of $H=102$ mm and total length of $L=300$ mm. Three typical electric heat sources (2) of $w=40$ mm length, $h=20$ mm height and 100 mm width are fixed in the base piece of the test section. The distance between the chips is equal $s=40$ mm, distance from entrance to the first heat source $L_1=40$ mm, and distance from the last heat source to the exit $L_2=40$ mm. The maximums power of heaters is 100 W and changed by Voltage transformer (Variac) (8). Ammeter (6) is used to measure the electric current, and then the value of the consumed power is evaluated from the measured values of voltage and current. More details about the test rig can be found in Kabeel et al. [17].

Two different fluids are used in this work; water and oil. Five thermocouples, J-type (3) of 0.25 mm diameter are fixed on the walls of each chip by high thermal conductivity epoxy to measure the temperature. The thermocouples are connected to a digital thermometer (5) type Emko-ESM 4430 with accuracy of $\pm 0.1^\circ\text{C}$. Fig.3 shows the thermocouples distribution on the chip.

The electric power to chips is turned on till the chips temperature reached steady state condition. Experimental results were taken every five minutes till the chip temperatures reach the steady state conditions.

The rate of heat generated through the electric resistance of the heater is equal to the heat transfer to the flowing air and is calculated by:

$$Q = IV \cos \phi \tag{1}$$

The average wall temperature of the tested body is defined as:

$$T_{w,avk} = \frac{\sum_{i=1}^n T_{wi}}{n} \tag{2}$$

Physical model

Fig. 2 shows a schematic diagram of the physical model. The heat sources (chips) are assumed to be of a constant heat flux and the enclosure having length L and height H, which represents the problem characteristic dimensions. The heat source is mounted on the bottom wall which is insulated and has dimensions $w \times h$. The sidewalls (right, top and left) of the enclosure are maintained at ambient temperature T_o .

Theoretical Model

The numerical model for the analysis is quite accurate and cost efficient compared to the experimental approach. On the other

hand, numerical simulation allows obtaining results faster than experimental when a hardware change is necessary. The two-dimensional steady-state, turbulent incompressible flow in the cabinet is governed by continuity, momentum and energy equations together with applying the turbulence $k-\epsilon$ model. The standard $k-\epsilon$ model and wall function are employed for the computations. The $k-\epsilon$ model is a semi-empirical model that has been proven to provide engineering accuracy in a wide spectrum of turbulent flows, including shear flow and wall-bounded flows.

The basic two-dimensional conservation equations are given as follows:

Continuity equation

$$\frac{\partial(\rho u)}{\partial x} + \frac{\partial(\rho v)}{\partial y} = 0 \tag{3}$$

Momentum equations:

$$\rho \left(u \frac{\partial u}{\partial x} + v \frac{\partial u}{\partial y} \right) = -\frac{\partial P}{\partial x} + \mu \nabla^2 u - \rho \left(\frac{\partial \overline{u'^2}}{\partial x} + \frac{\partial \overline{u'v'}}{\partial y} \right) \tag{4}$$

$$\rho \left(u \frac{\partial v}{\partial x} + v \frac{\partial v}{\partial y} \right) = -\frac{\partial P}{\partial y} + \mu \nabla^2 v - \rho \left(\frac{\partial \overline{u'v'}}{\partial x} + \frac{\partial \overline{v'^2}}{\partial y} \right) \tag{5}$$

Energy equation:

$$u \frac{\partial T}{\partial x} + v \frac{\partial T}{\partial y} = \left(\alpha + \frac{\nu_t}{\sigma_t} \right) \nabla^2 T + \mu \phi + S_r \tag{6}$$

Turbulence energy equation:

$$u \frac{\partial k}{\partial x} + v \frac{\partial k}{\partial y} = \left(\nu + \frac{\nu_t}{\sigma_k} \right) \left(\frac{\partial^2 k}{\partial x^2} + \frac{\partial^2 k}{\partial y^2} \right) - (\nu + \nu_t) C_1 G \epsilon - \beta g \frac{\nu_t}{\sigma_k} \frac{\partial T}{\partial y} - \epsilon \tag{7}$$

Turbulence dissipation rate equation:

$$u \frac{\partial \varepsilon}{\partial x} + v \frac{\partial \varepsilon}{\partial y} = \left(u + \frac{v}{\sigma_k} \right) \left(\frac{\partial^2 \varepsilon}{\partial x^2} + \frac{\partial^2 \varepsilon}{\partial y^2} \right) - \left(C_{1\beta} g \varepsilon \frac{v_i}{\sigma_k} \frac{\partial T}{\partial y} - C_2 \varepsilon^2 \right) / k + \left(u + \frac{v}{\sigma_k} \right) C_1 G \varepsilon \quad (8)$$

Where:

$$G = 2 \left[\left(\frac{\partial u}{\partial x} \right)^2 + \left(\frac{\partial v}{\partial y} \right)^2 \right] + \left(\frac{\partial u}{\partial y} + \frac{\partial v}{\partial x} \right)^2 \quad (9)$$

The turbulent kinematic viscosity is:

$$\nu_T = C_\mu \frac{k^2}{\varepsilon} \quad (10)$$

Where the turbulence dissipation rate is given by:

$$\varepsilon = C_D \frac{k^2}{\ell} \quad (11)$$

The k-ε model constants C_μ , C_1 , C_2 , σ_k , and σ_ε values are presented in table (1).

Table (1): The standard values of k-ε model constants [18].

C_μ	C_1	C_2	σ_k	σ_ε
0.09	1.44	1.92	1	1.3

The local Nusselt number (Nu) along the surface of the chips may be expressed with the local heat transfer coefficient as:

$$Nu(X) = \frac{h d}{\lambda_f} = \frac{l}{\theta_w} \quad (12)$$

Where "n" is the coordinate normal to the surface of chips.

The average surface Nusselt number (\overline{Nu}) on chips is calculated with expression

$$Nu_m = \frac{1}{A} \int_A Nu dA \quad (13)$$

Where A is the surface area exposed to the fluid.

Boundary conditions

The boundary conditions of above governing equations for the considered problem as shown in Fig. 3 are determined as:

On solid walls (Chips and enclosure): No-slip condition is applied for velocities, i.e., $u = v = 0$.

The thermal condition on cooling walls of enclosure (right, top and left) are $T = T_0$

On adiabatic bottom walls (Chips and enclosure) are $Q = 0$

On heat source walls (right, top and left) are $q'' = C$

Numerical solution

After setting the governing equations, a numerical technique is used to convert them into a set of algebraic equations. Then, the computational fluid dynamics "Fluent 6.3.26" based on the SIMPLE algorithm, [18], is introduced to simulate the problem under consideration.

Results and discussion

In the present study, the effect of the heat flux on the cooling process is studied. During the study, the heat flux varied from 100 to 800 W/m² for water, whereas two values of the heat rate (100 and 200 W/m²) are examined for dielectrics oil. The properties of water and dielectrics oil are given in table 2

Table (1): The properties of water and dielectrics oil.

Type	ρ Kg/m ³	C_p kJ/kg.K	λ W/m.k	μ Kg/m.s
water	1000	4.182	0.6	0.001
oil	953	1.81	0.101	0.05

Theoretical results

The present numerical model is used for the case of natural convection flow from three generating heat sources. The

theoretical results of the system used are obtained at different conditions for water and dielectrics oil.

Theoretical results using water

The temperature fields and the chips surface temperature are illustrated in Figs. 4-8 at 100, 200, 400, 600 and 800 W/m². The maximum surface temperature (hot spot) on the discrete chip is seen to occur at the top row because fluid motion is weak and the local bulk fluid temperature is high in the ceiling. On the other hand, the chip surface temperature has the lowest value at the bottom row where the local bulk fluid temperature is the lowest. The maximum surface temperature is found at chip 2 and is about 35, 45, 65, 85, 97 °C at 100, 200, 400, 600 and 800 W/m² respectively. It can be seen that the temperature of chip 2 has higher value than the chips 1 and 3.

From Figs. 4-8, it is found that the isotherm gradient of fluid is higher near the chip faces, and increases with increasing heat flux due to increased buoyancy effects. The temperature gradient of fluid on the rear-side of the chip is very large and hence heat loss is quite considerable from the chip. With increasing heat flux, the primary and secondary cells are reduced in size due to increased heat transfer rates to the enclosure walls. The larger cell breaks into multiple smaller cells at higher heat flux. On comparing isotherm contours for different heat fluxes, it is found that the trends are altered considerably as expected. The surface temperature of right and left for the discrete chip 2, are the same. The surface temperature of right discrete chip 1 and left discrete chip 3 are the same. Also, the surface temperature of left discrete chip 1 and right discrete chip 3 are the same.

Theoretical results using dielectrical oil

The temperature fields and the chips surface temperature using dielectrical oil at

different heat fluxes 100 and 200 W/m² are shown in Figs. 9 and 10. It can be seen that the temperature of chip 2 has higher value than the chip 1 and 3. It can be observed that the trend of all curves is the same as that for water. In Comparison with water cooling, the temperatures of chips 1, 2 and 3 are larger when oil is used as coolant, which means that better cooling could be obtained when water is used. The maximum surface temperature is found at chip 2 (about 60, 95 °C) at heat rates of 100, 200 W/m², respectively.

Relationship between the average surface nusselt number and heat flux

Fig. 11 presents the relationship between the average surface nusselt number (Nu) and heat flux (q'') for using water. The average surface nusselt number increases with the increase heat flux and average surface nusselt number for chip 2 is lower than that chip 1 and 3. The following empirical formal between Nu and q'' can be obtained from the theoretical data:

$$Nu = 6.515 + 0.03 q'' - 2.084 q''^2 \pm 4 \quad (14)$$

Comparison between theoretical and experimental results using water and dielectrical oil

The average surface temperature of the experimental and theoretical as a function of time for the three chips is shown in Figs. 12 and 13. It can be observed that the average wall temperature of chips increase with the time increase for all chips. The difference between the theoretical and experimental results can be explained for the some assumption in the theoretical model. The approximated agreement between the experimental measured and calculated average wall temperature of chips is good and the shift between results is percentage difference average 4.1% for water at 200 W/m² and 3.5% for dielectrical oil at 200 W/m².

CONCLUSION

Natural convection heat transfer from discrete heat sources mounted in rectangular enclosure using liquid coolant is studied theoretically and experimentally. From the theoretical and experimental results, it can be concluded that:

- Heat transfer from discrete heaters is non-uniform and should be accounted for by applying the averaging techniques.
- Maximum heat transfer occurs at the heater leading and side edges.
- The heater surface temperature is the highest at the top-row heaters.
- Compared with oil, water gives good cooling results.
- The larger cell breaks into multiple smaller cells at higher heat fluxes.
- Good agreement between theoretical and experimental results is found.

Nomenclature

C_o	Outlet fluid velocity, m/s
C_1, C_2	Empirical constants, -
C_D, C_μ	Empirical constants, -
C_p	Constant pressure specific heat, J/kg.K
$\cos \varphi$	Power factor, -
g	Gravitational acceleration, m/s ²
I	Electric current, A
k	Turbulence kinetic energy, J/kg
n	Number of thermocouples, -
Nu	The local Nusselt number
\overline{Nu}	The average surface Nusselt number
P	Pressure, kPa
Q	Rate of heat generation, W
S_T	Temperature source term, W/m ³
T	Temperature
$T_{m,t}$	Average temperature, K
T_o	Ambient temperature, K
u	Velocity component in x-direction, m/s
V	Applied voltage, V

V	Electrical potential difference, V
v	Velocity component in y-direction, m/s
x, y	Coordinates

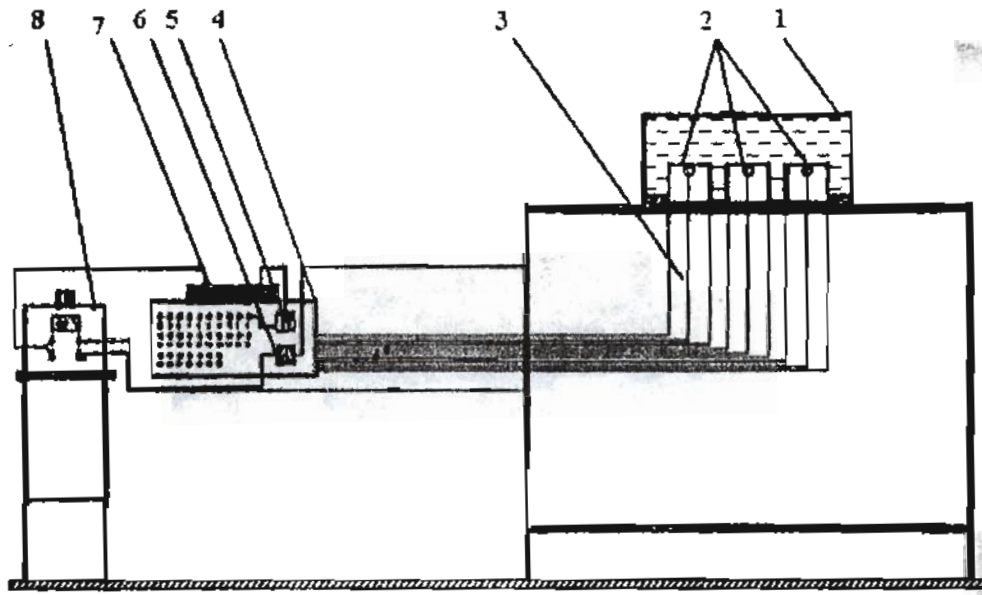
Greeks:

α	Thermal diffusivity, m ² /s
β	Thermal expansion coefficient, K ⁻¹
ρ	Air density, kg/m ³
ε	Turbulent energy dissipation rate, W/kg
ν	Kinematic viscosity, m ² /s
λ	Thermal conductivity, W/m.K
σ	Diffusion coefficient, m ² /s
μ	Dynamic viscosity, kg/m.s

References

- [1] S. Mohapatra and D Loikits, Advances in Liquid Coolant Technologies for Electronics Cooling, Proceedings of the 21st IEEE Semiconductor Thermal Measurement and Management Symposium, San Jose, CA, 2005, pp. 354-360.
- [2] M. Mahalingam, H. Berg, Thermal trend in component level packaging, Int. J. Hybrid Microelectron. 7 (1984) 1-9.
- [3] R. Simon, Thermal management of electronic packages, Solid State Technol. 26(1983) 131-137.
- [4] Po-C. Huang, C.-Fu Yang, Analysis of pulsating convection from two heat sources mounted with porous blocks, International Journal of Heat and Mass Transfer 51 (2008) 6294-6311
- [5] C. Linhui, T. Huaizhang, L. Yanzhong, Z. Dongbin, Experimental study on natural convective heat transfer from a vertical plate with discrete heat sources mounted on the back, Energy Conversion and Management 47 (2006) 3447-3455
- [6] C. T. Nguyen, G. Roy, C. Gauthier, N. Galanis, Heat transfer enhancement

- using Al_2O_3 water nanofluid for an electronic liquid cooling system, *Applied Thermal Engineering* 27 (2007) 1501–1506
- [7] W.W. Wits, T.H.J. Vaneker, J.H. Mannak, R. Legtenberg, Novel cooling strategy for electronic packages: Directly injected cooling, *CIRP Journal of Manufacturing Science and Technology* (2008)
- [8] G. P. XU, K. W. TOU and C. P. TSO, Numerical modeling of turbulent heat transfer from discrete heat sources in a liquid-cooled channel, *Int. J. Heat Mass Transfer*. Vol. 41, No. 10, pp. 1157–1166, 1998
- [9] L.F. Jin , K.W. Tou , C.P. Tso , Effects of rotation on natural convection cooling from three rows of heat sources in a rectangular cavity, *International Journal of Heat and Mass Transfer* 48 (2005) 3982–3994
- [10] G.V. Kuznetsov, M.A. Sheremet, Conjugate heat transfer in an enclosure under the condition of internal mass transfer and in the presence of the local heat source, *International Journal of Heat and Mass Transfer* 52 (2009) 1–8
- [11] H. Bhowmik, C.P. Tso, K.W. Tou, F.L. Tan, Convection heat transfer from discrete heat sources in a liquid cooled rectangular channel, *Applied Thermal Engineering* 25 (2005) 2532–2542
- [12] R. N. Mathews, C. Balaji, Numerical simulation of conjugate, turbulent mixed convection heat transfer in a vertical channel with discrete heat sources, *International Communications in Heat and Mass Transfer* 33 (2006) 908–916
- [13] A. Dogan , M. Sivrioglu , S. Baskaya, Investigation of mixed convection heat transfer in a horizontal channel with discrete heat sources at the top and at the bottom, *International Journal of Heat and Mass Transfer* 49 (2006) 2652–2662
- [14] A. Rivas-Cardona, A. Hernandez-Guerrero, R. Romero-Méndez, R. Lesso-Arroyo, Liquid-mixed convection in a closed enclosure with highly-intensive heat fluxes, *International Journal of Heat and Mass Transfer* 47 (2004) 4089–4099
- [15] J. Kim, Spray cooling heat transfer: The state of the art, *International Journal of Heat and Fluid Flow* 28 (2007) 753–767
- [16] A.S. Huzayyin, S.A. Nada, M.A. Rady, A. Faris, Cooling an array of multiple heat sources by a row of slot air jets, *International Journal of Heat and Mass Transfer* 49 (2006) 2597–2609
- [17] A. E. Kabeel, A. Khalil and F. Eldosary, Liquids cooling of electronic heat sources, *Mansoura Engineering Journal*, March 2009
- [18] S. V Patankar, "Numerical Heat Transfer and Fluid Flow", Hemisphere Publishing Company, New York, 1980



- | | |
|---------------------|---------------------------------|
| 1- Cooling chamber. | 5- Temperature indicator |
| 2- Chips. | 6- Ammeter |
| 3- Thermocouples | 7- AC electric source |
| 4- Control panel. | 8- Voltage transformer (Varicc) |

Fig. 1. Schematic diagram of the experimental test rig

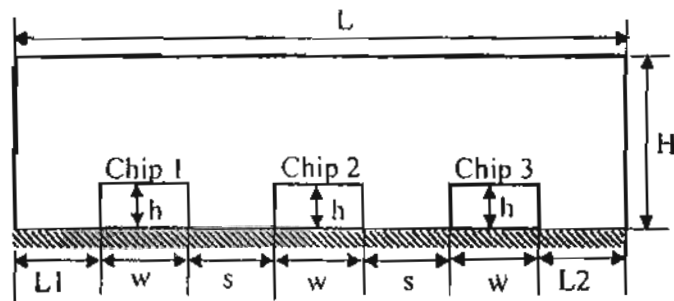


Fig. 2. Schematic diagram of physical configuration

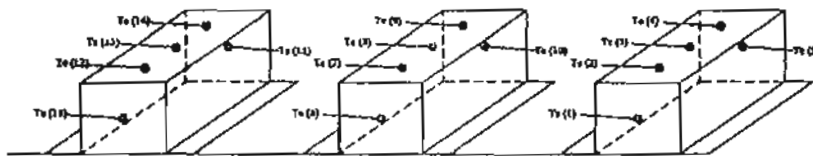


Fig. 3. Thermocouples distribution

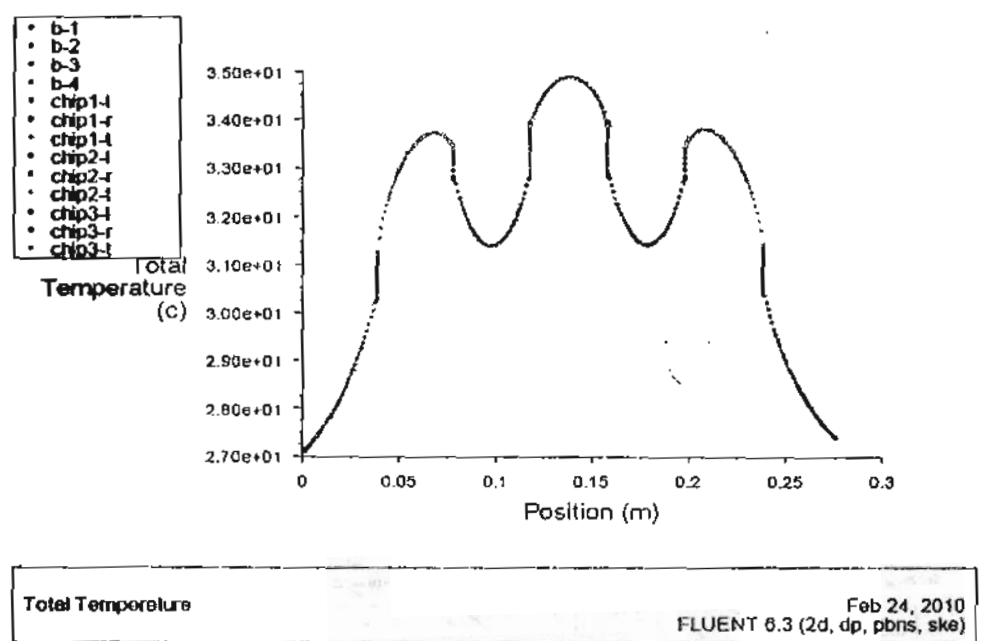
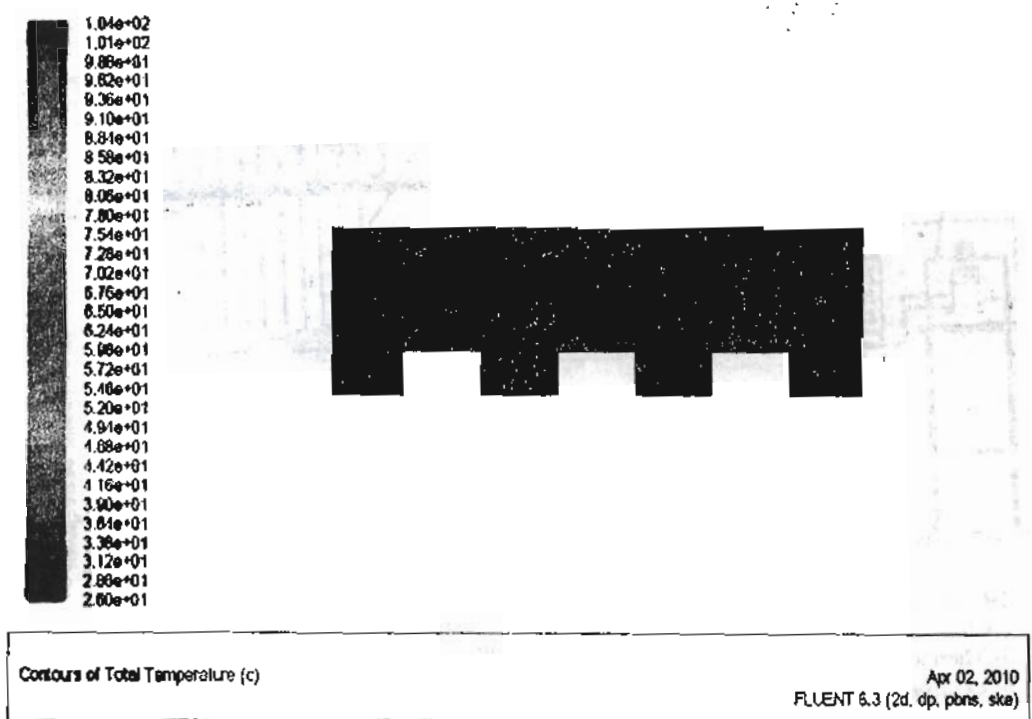
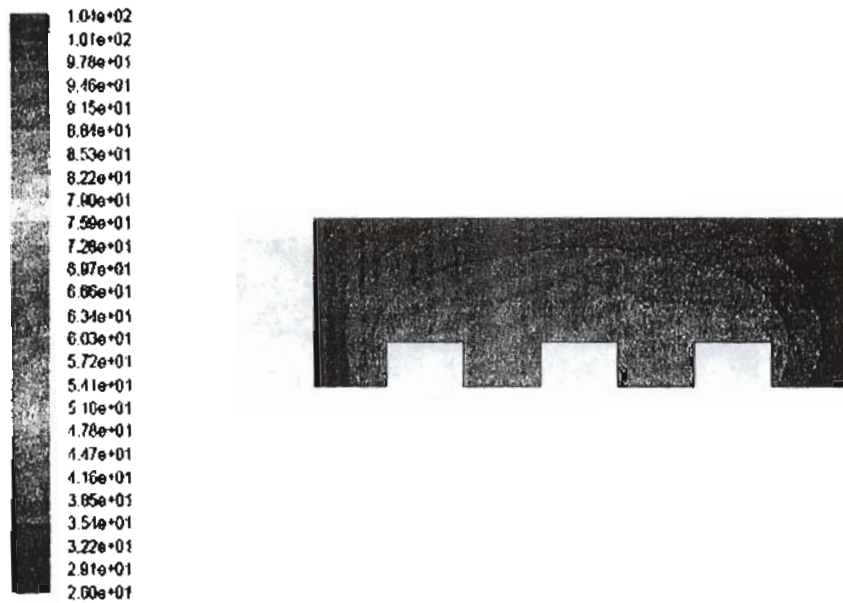
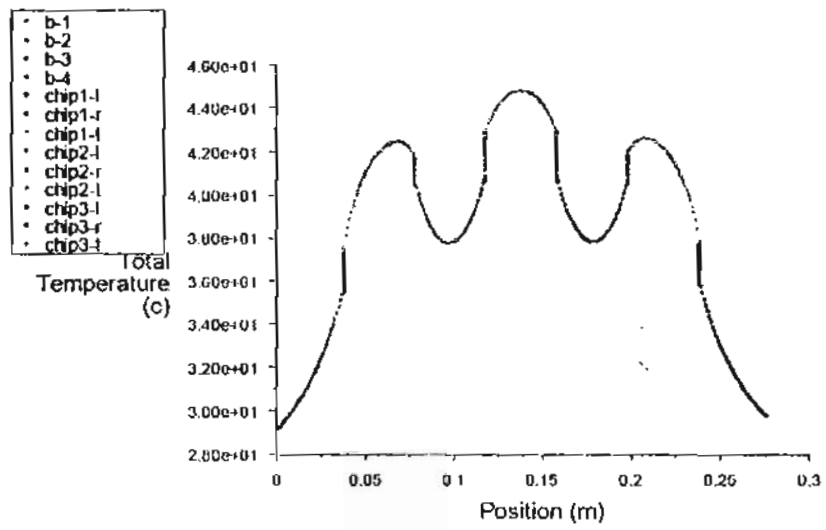


Fig. 4. The temperature contours and the chips surface temperature using water at heat flux 100 W/m^2



Contours of Total Temperature (c) Apr 02, 2010
FLUENT 6.3 (2d, dp, pbrns, ske)



Total Temperature Feb 24, 2010
FLUENT 6.3 (2d, dp, pbrns, ske)

Fig. 5. The temperature contours and the chips surface temperature using water at heat flux 200 W/m^2

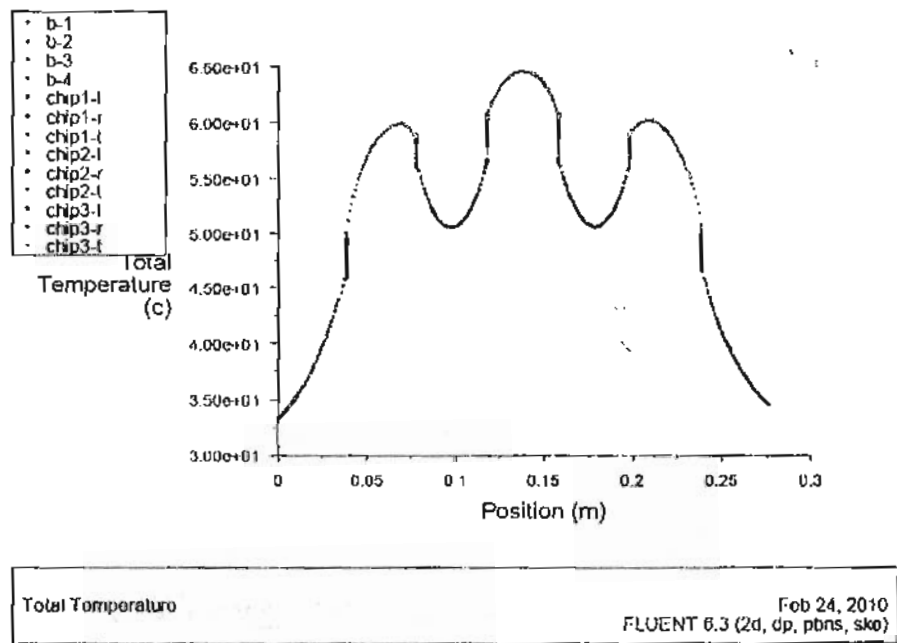
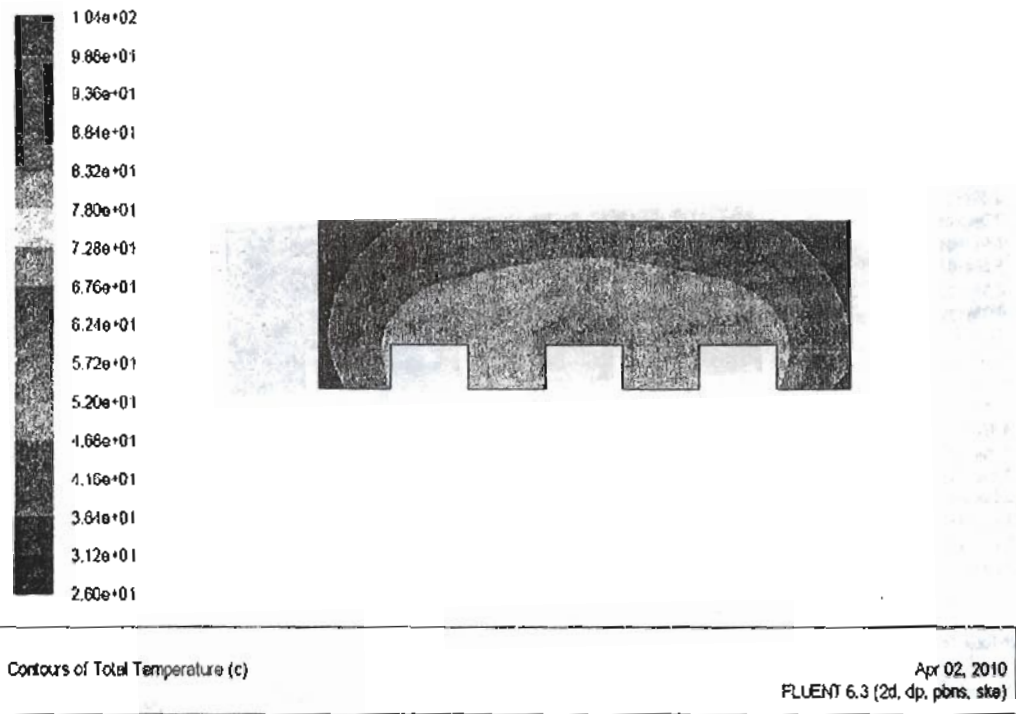


Fig. 6. The temperature contours and the chips surface temperature using water at heat flux 400 W/m^2

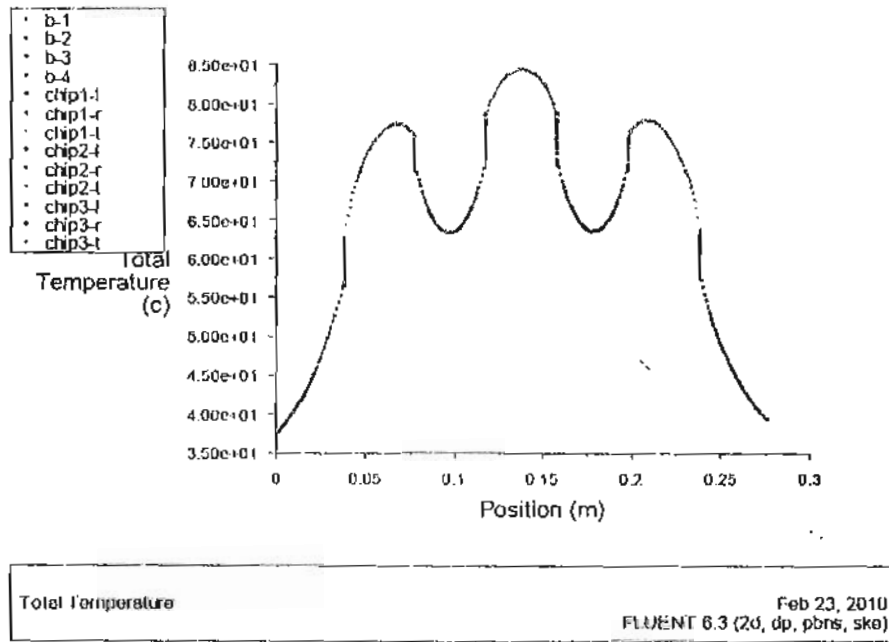
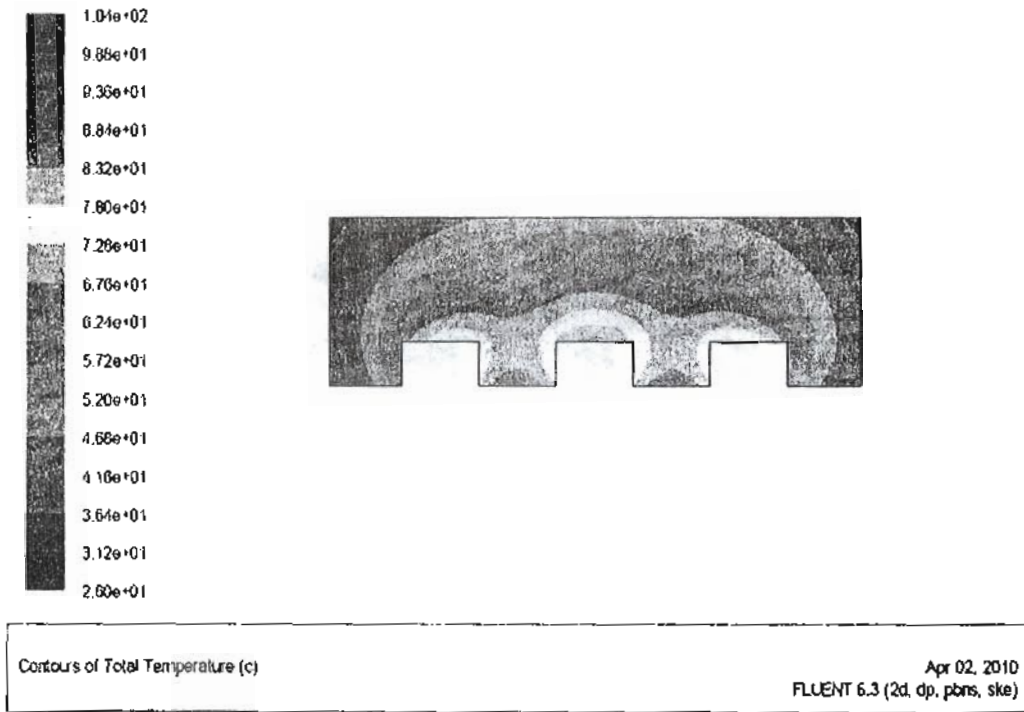


Fig. 7. The temperature contours and the chips surface temperature using water at heat flux 600 W/m^2

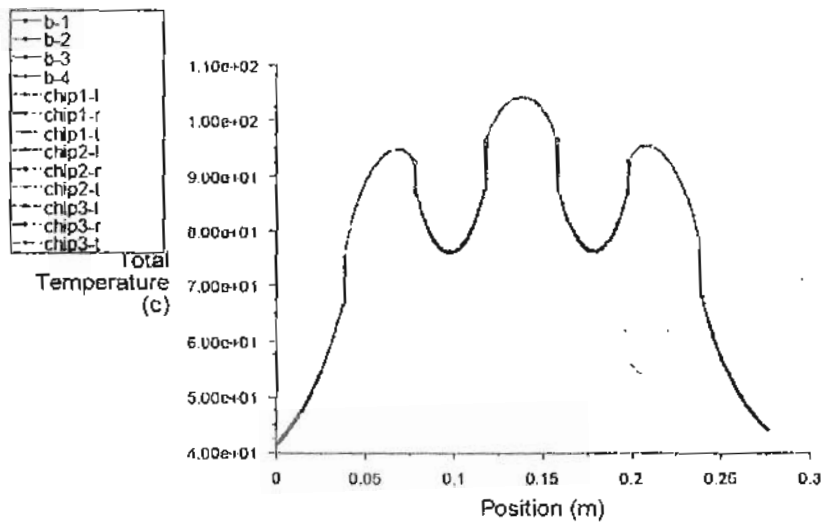
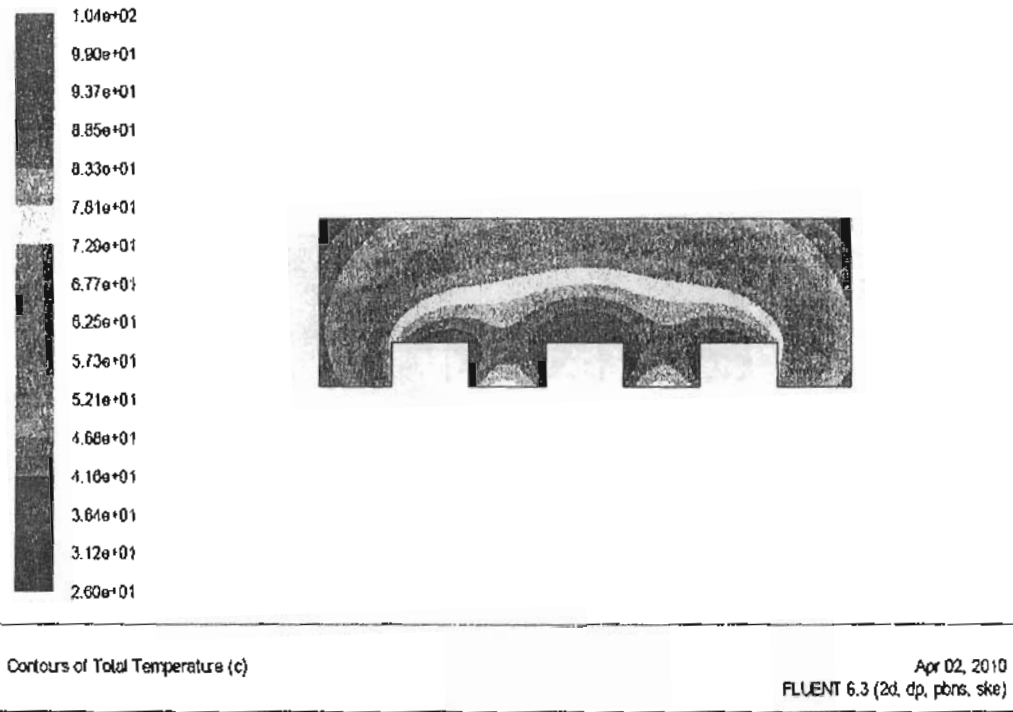


Fig. 8. The temperature contours and the chips surface temperature using water at heat flux 800 W/m^2

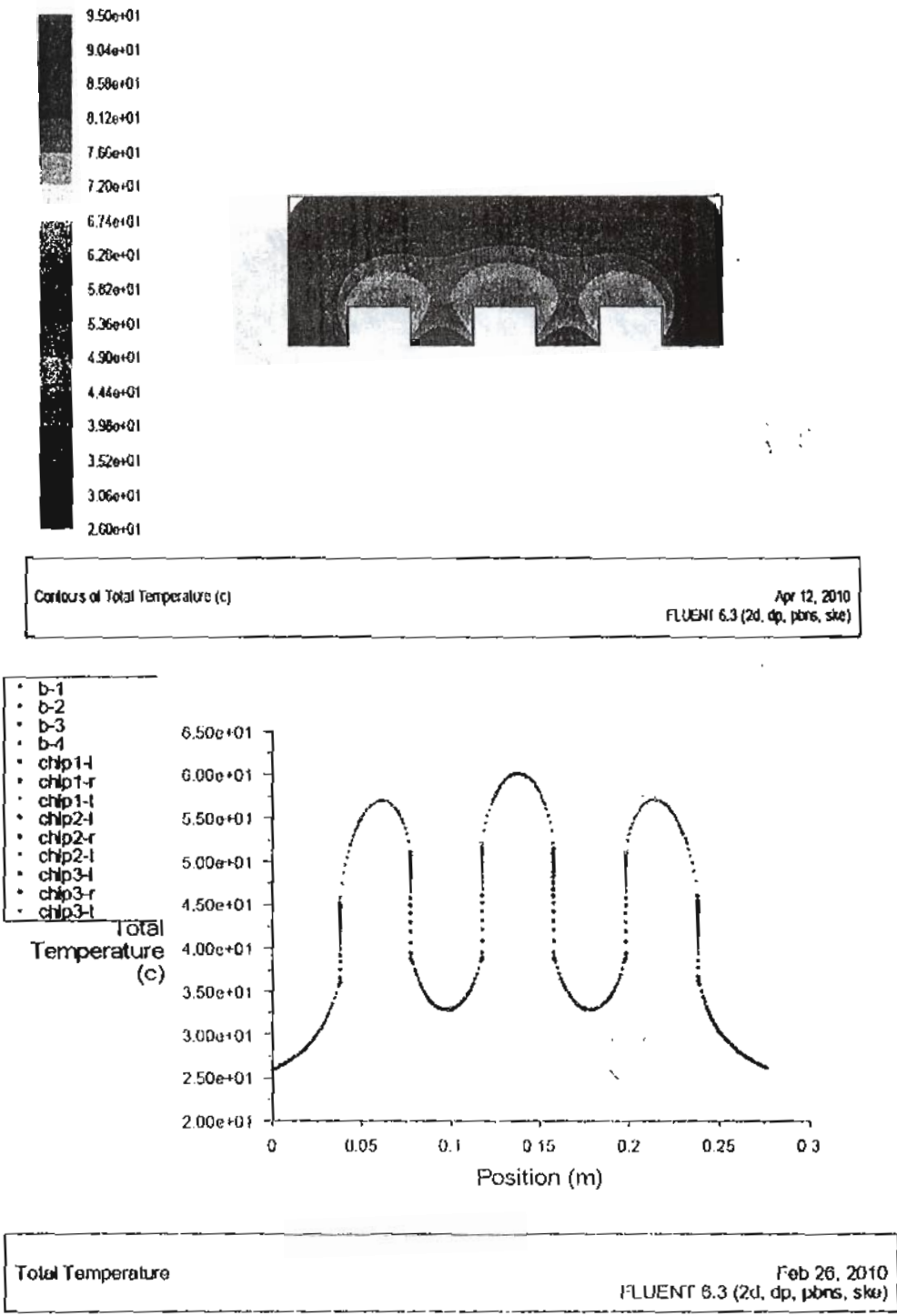
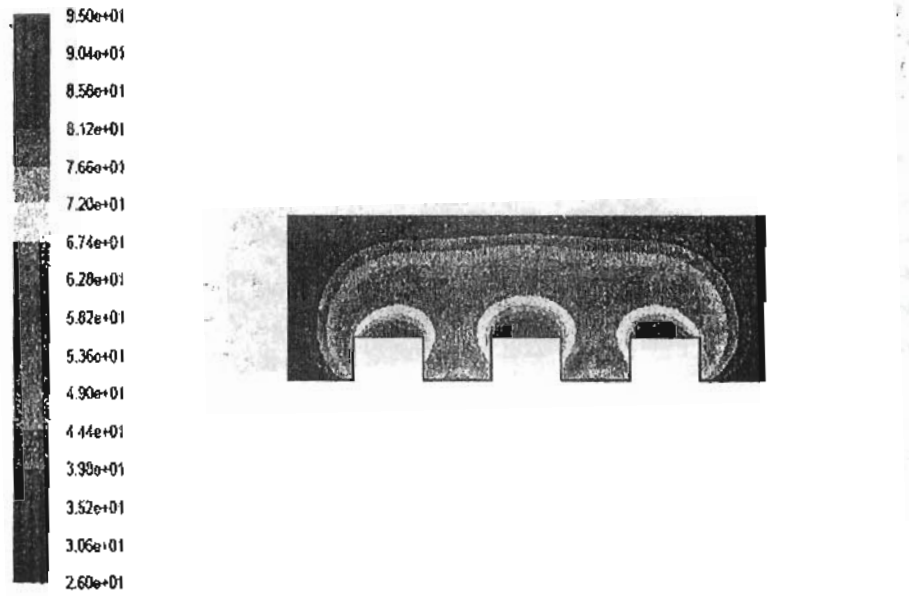
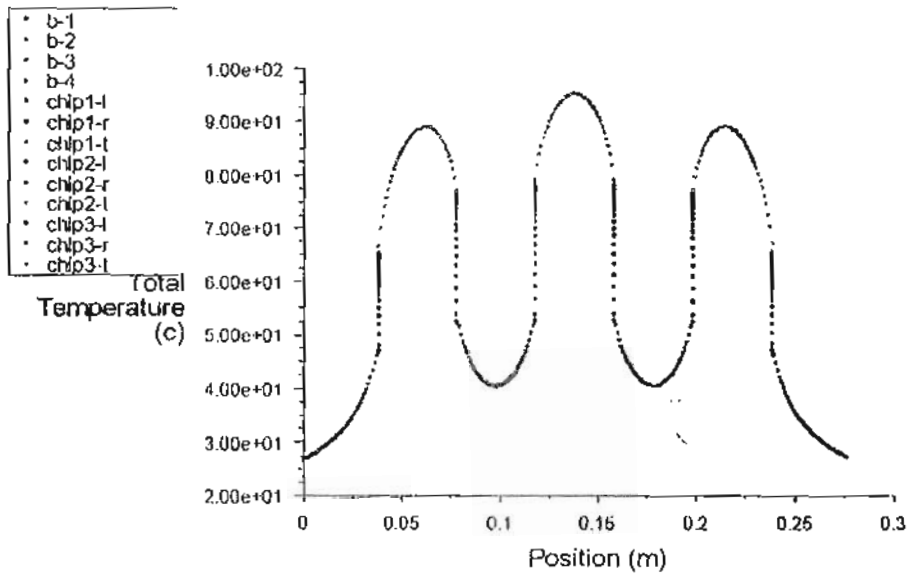


Fig. 9. The temperature contours and the chips surface temperature using dielectrical oil at heat flux 100 W/m²



Contours of Total Temperature (c) Apr 12, 2010
FLUENT 6.3 (2d, dp, pbns, ske)



Total Temperature Feb 26, 2010
FLUENT 6.3 (2d, dp, pbns, ske)

Fig. 10. The temperature contours and the chips surface temperature using dielectrical oil at heat flux 200 W/m²

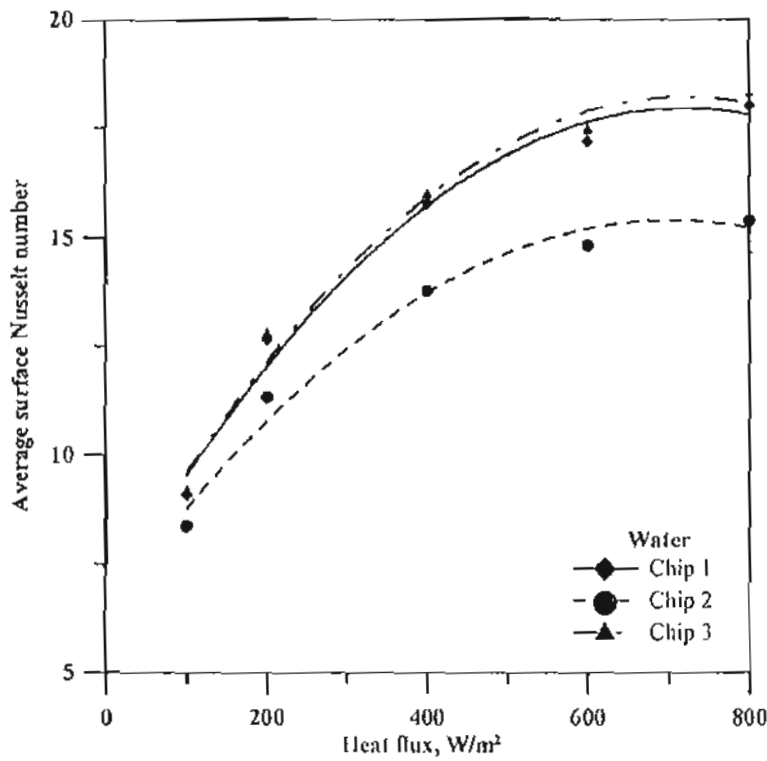


Fig. 11. The relationship between the average surface nusselt number and heat flux for water

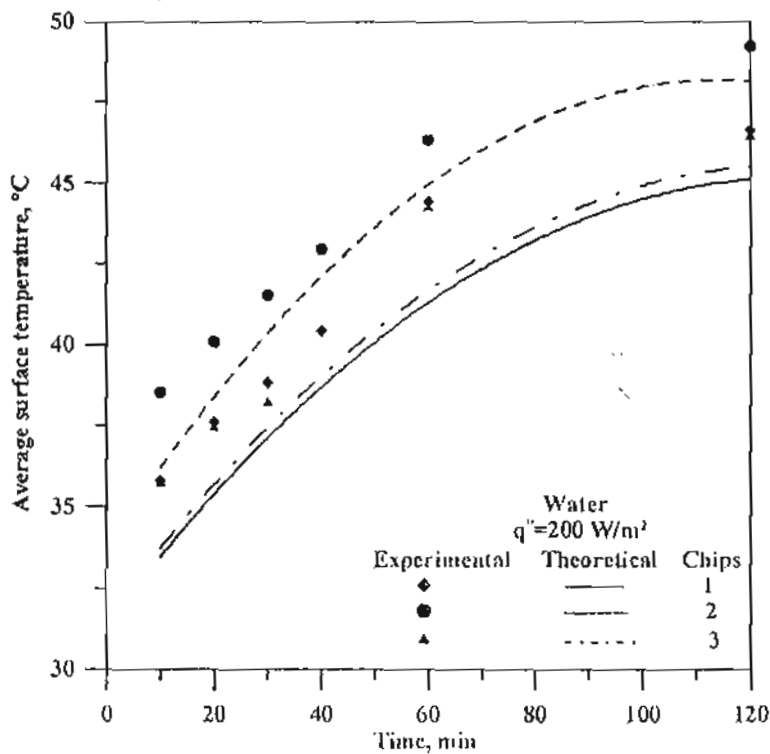


Fig. 12. Average wall temperature versus time for water cooled chips.

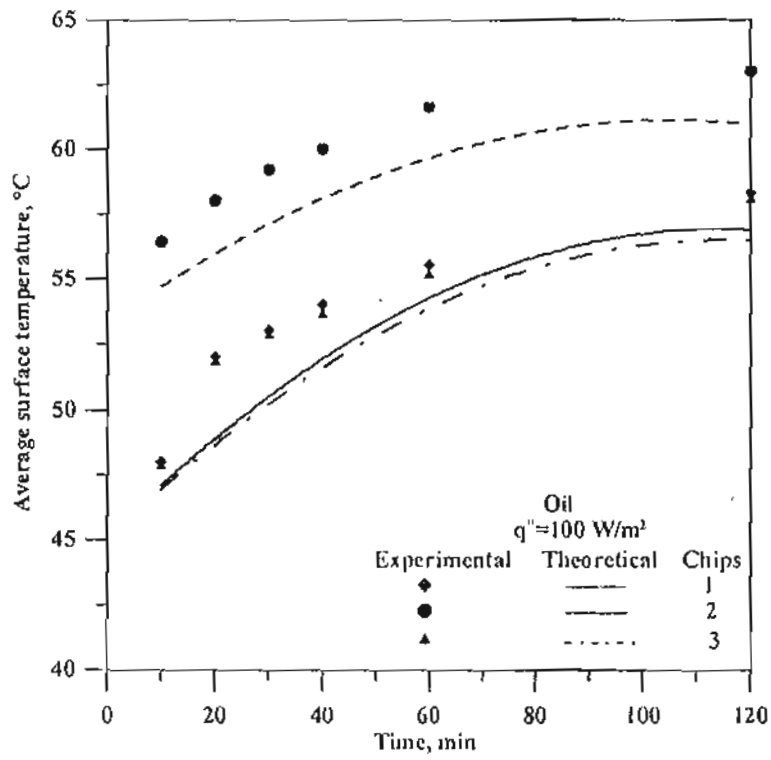


Fig. 13. Average wall temperature versus time for oil cooled chips.